RESEARCH ARTICLE

Obesity, Diabetes and Energy Homeostasis

Lipid oxidation during thermogenesis in high-altitude deer mice (*Peromyscus maniculatus*)

Sulayman A. Lyons,[1] Kevin B. Tate,[1] Kenneth C. Welch Jr.,[2] and ⦿ Grant B. McClelland[1]

[1]*Department of Biology, McMaster University, Hamilton, Ontario, Canada and* [2]*Department of Biological Sciences, University of Toronto Scarborough, Toronto, Ontario, Canada*

Abstract

When at their maximum thermogenic capacity (cold-induced $\dot{V}o_{2max}$), small endotherms reach levels of aerobic metabolism as high, or even higher, than running $\dot{V}o_{2max}$. How these high rates of thermogenesis are supported by substrate oxidation is currently unclear. The appropriate utilization of metabolic fuels that could sustain thermogenesis over extended periods may be important for survival in cold environments, like high altitude. Previous studies show that high capacities for lipid use in high-altitude deer mice may have evolved in concert with greater thermogenic capacities. The purpose of this study was to determine how lipid utilization at both moderate and maximal thermogenic intensities may differ in high- and low-altitude deer mice, and strictly low-altitude white-footed mice. We also examined the phenotypic plasticity of lipid use after acclimation to cold hypoxia (CH), conditions simulating high altitude. We found that lipids were the primary fuel supporting both moderate and maximal rates of thermogenesis in both species of mice. Lipid oxidation increased threefold in mice from 30°C to 0°C, consistent with increases in oxidation of [13C]palmitic acid. CH acclimation led to an increase in [13C]palmitic acid oxidation at 30°C but did not affect total lipid oxidation. Lipid oxidation rates at cold-induced $\dot{V}o_{2max}$ were two- to fourfold those at 0°C and increased further after CH acclimation, especially in high-altitude deer mice. These are the highest mass-specific lipid oxidation rates observed in any land mammal. Uncovering the mechanisms that allow for these high rates of oxidation will aid our understanding of the regulation of lipid metabolism.

cold-induced $\dot{V}o_{2max}$; fat oxidation; substrate utilization; summit metabolism

INTRODUCTION

Homeothermic endothermy is a distinctive feature of mammals that is crucial for their survival in cold environments. However, thermal tolerance and thermogenic capacity are performance traits that not only vary with body size but also with individual and population differences in thermal history (1–3). For instance, small mammals have greater thermoregulatory costs compared with larger species due to a higher surface area for heat loss relative to volume used for heat production. This can be especially challenging for species that are active during colder parts of the year, necessitating high rates of thermogenesis to remain active when temperatures are low (4, 5). Past research has uncovered many details on how these species can maintain high rates of O_2 delivery to thermogenic tissues (6). However, it remains unclear how metabolic substrates are utilized to support high rates of thermogenesis in mammals or if fuel use patterns change seasonally.

Thermogenesis is an aerobic process that allows endotherms to maintain stable body temperatures by balancing heat lost to the external environment with endogenous heat production. The onset of thermogenesis occurs when the ambient temperature falls below an endotherm's thermoneutral zone (3) and can occur in two major ways, shivering and nonshivering thermogenesis (NST). Shivering thermogenesis increases metabolic demand via muscular contractions that provide heat but no beneficial locomotory work, whereas NST produces heat through the futile cycling of protons across the mitochondrial membrane via uncoupling protein 1 in brown adipose tissue (BAT) (7). Although shivering is fueled by both carbohydrates and lipids, depending on shivering intensity (8), NST is primarily fueled by lipids (9, 10). Furthermore, prolonged cold exposure increases shivering capacity (11) and elevates BAT metabolic activity (12, 13).

Endogenous lipid stores are large in mammals (∼80% of the available energy reserves), and it has been speculated that lipids may be used to sustain heat production (14). Data from rats show that during modest cold exposure (5°C), lipid oxidation supports over 50% of the metabolic demand of shivering thermogenesis (15). However, we are not aware of any study examining fuel use for thermogenesis in smaller

R735

mammals, such as mice. It is well-characterized in mammals that maximal rates of lipid oxidation during locomotion occur at moderate intensities of aerobic exercise (16–18), and these rates do not vary even if fat availability is artificially elevated (19). Although during exercise higher mass-specific rates of lipid oxidation are observed in mice compared with larger species, they too demonstrate an upper limit to lipid use at submaximal exercise intensities (17, 20, 21). Interestingly, during cold-induced $\dot{V}_{O_{2max}}$ (also referred to as summit metabolism), small endotherms often reach levels of aerobic metabolism higher than $\dot{V}_{O_{2max}}$ elicited by exercise (4, 22, 23). This suggests that metabolism supporting even moderate rates of thermogenesis may be higher than those during aerobic exercise, when lipid oxidation plateaus or even declines (24). Whether small mammals can sustain sufficient rates of lipid oxidation to support even these moderate rates of thermogenesis is unclear.

High-altitude environments can be cooler year-round than lower elevations of the same latitude. Yet, populations of small mammals native to high altitude, such as deer mice, remain active in the cold, maintaining higher daily energetic costs compared with low altitude conspecifics, even during summer months (5). There is also evidence of directional selection for greater cold-induced $\dot{V}_{O_{2max}}$ in deer mice at high altitude (25), and thermogenic capacity in hypoxia is higher in high-altitude deer mice compared with lowland conspecifics (26–28). This superior aerobic capacity at high altitude is the product of environmentally induced phenotypic plasticity overlaid upon fixed population differences (27, 29, 30). Although the oxygen transport pathway from the external environment to muscle tissues has been extensively examined in mammals living at high altitude (31), fuel use has received much less attention. However, work examining exercise metabolism in high altitude conditions suggests a greater reliance in carbohydrates to support submaximal locomotion, presumably as an oxygen-saving strategy. This has been demonstrated in two species in the genus *Phyllotis* native to the high Andes (17) and in deer mice native to the Rocky Mountains, born and raised at low altitude and acclimated to chronic hypoxia (20). However, how metabolic fuel use may have evolved at altitude to support the high rates of thermogenesis is currently not well understood.

It would be unlikely that a preferential utilization of carbohydrate oxidation occurs to support the high rates of thermogenesis at high altitude, given mammals have limited glycogen reserves (23), and the prolonged nature of thermoregulation would quickly deplete these stores. Indeed, after a 6-wk acclimation to low altitude conditions, wild high-altitude native deer mice showed respiratory exchange ratios (RER = $\dot{V}_{CO_2}/\dot{V}_{O_2}$) at cold-induced $\dot{V}_{O_{2max}}$ in hypoxia suggestive of a high reliance on lipids (26). These high proportions of lipid use may be largely influenced by NST activity in BAT. Moreover, the higher thermogenic capacities in high-altitude mice suggest a corresponding elevated rate of lipid oxidation. Phenotypic differences between low- and high-altitude deer mice in the gastrocnemius, a muscle used in thermogenesis (32), suggest higher capacities for fatty acid oxidation at high altitude, presumably to support high rates of shivering (20, 26).

Whether moderate and/or maximal rates of heat production are supported solely by lipids or a combination of metabolic fuels has not been explored in either low or high-altitude deer mice. Moreover, it is unclear if lipid oxidation rates follow the same population differences in aerobic capacity, or if this fuel utilization for heat production is affected by acclimation to simulated high-altitude conditions.

To address these issues, we used deer mice (*Peromyscus maniculatus*) native to high altitude and compared them with a low-altitude population and to a closely related strictly low-altitude species, the white-footed mouse (*P. leucopus*). Mice were born and raised in common low-altitude conditions and acclimated as adults to cold hypoxia simulating high altitude. We tested the hypothesis that moderate and maximal rates of thermogenesis are predominately supported by lipid metabolism in deer mice and rates of lipid oxidation are higher in deer mice native to high altitude. High-altitude deer mice are also predicted to respond to chronic cold hypoxia with a greater increase in lipid oxidation during thermogenesis than low-altitude mice.

MATERIALS AND METHODS

Animals and Experimental Design

Male and female deer mice and white-footed mice used in this study were first-generation descendants of wild-caught *Peromyscus maniculatus rufinus* trapped at the summit of Mount Evans, CO (4,350 m a.s.l.), and *Peromyscus maniculatus nebracensis* and *Peromyscus leucopus* trapped at low altitude at Nine-mile Prairie, NE (320 m a.s.l.). Mice were born and raised at McMaster University ($\sim$90 m a.s.l.) under common laboratory conditions of $\sim$23°C, light cycle of 12:12 h light:dark, food, and water ad libitum. All mice were at least 6 mo of age before the start of experiments. This experimental design allows us to separate the effects of altitude ancestry and environment on physiological traits (20, 26, 29, 30). All procedures were approved by the McMaster University Animal Research Ethics Board in accordance with guidelines from the Canadian Council on Animal Care.

Acclimation Conditions

First-generation high-altitude (HA) and low-altitude (LA) deer mice were randomly divided into two acclimation groups and kept for 6 to 8 wk in either, *1*) warm normoxia (WN), at 23°C and 760 mmHg (21 kPa O_2)—our common laboratory conditions, or *2*) cold hypoxia (CH), at 5°C and 480 mmHg (12 kPa O_2) using hypobaric chambers (33) housed in a climate controlled room to simulate an altitude of 4,300 m a.s.l. Mice in the CH group were first placed in a cold room for 24 h at normobaria to adjust to the cold before being placed in the hypobaric chambers. Mice in CH were returned to normobaria in cold for a brief period (<1 h) twice a week to clean cages and replenish food and water (28, 30).

Respirometry

Open-flow respirometry was used to determine rates of oxygen consumption ($\dot{V}_{O_2}$) and CO_2 production ($\dot{V}_{CO_2}$). For each mouse, $\dot{V}_{O_2}$ and $\dot{V}_{CO_2}$ were measured at thermoneutral temperatures (30°C) (34) and moderate cold temperatures (0°C) using a PTC-1 portable controlled-temperature cabinet (Sable Systems, Las Vegas, NV) in random order. Mice were

made postabsorptive by a 4–6 h fast, weighed, and placed in a respirometry chamber (~500 mL). Dry (Drierite, Hammond, OH) and CO_2-free (Soda Lime and Ascarite, Thomas Scientific, NJ) air was flowed (pushed) into the respirometry chamber at 600 mL/min, using a mass-flow controller (Sable Systems). Excurrent air was subsampled at a rate of ~200 mL/min, dried using prebaked Drierite (35), and passed through O_2 and CO_2 analyzers (Sable Systems). Fractional incurrent O_2 (FI_{O_2}) and CO_2 (FI_{CO_2}) were recorded at the beginning and end of the trial by flowing air through an empty respirometry chamber. After mice adjusted to the chamber for 20 min, fractional excurrent concentrations of O_2 (FE_{O_2}) and CO_2 (FE_{CO_2}) were determined for 20 min, and $\dot{V}O_2$ and $\dot{V}CO_2$ were calculated using *Eq. 3b* from Withers (36). Body temperatures were measured before and after all experimental trials using a rectal probe thermometer (RET-3-ISO, Physitemp). Resting $\dot{V}O_2$ was defined as the lowest, most stable reading during a 1.5-min interval during the last 20 min of the trial. Whole animal rates of substrate oxidation were calculated using the indirect calorimetry equations from Frayn (37) assuming a minimal contribution of protein oxidation in the postabsorptive state (38, 39). Protein oxidation has been shown to contribute only ~5% to energy production during exercise in postabsorptive mammals. Thus, we assumed no contribution of protein oxidation when calculating rates of fuel oxidation. Thermal conductance (C) was calculated based on equations from Scholander et al. (3).

Hypoxic cold-induced $\dot{V}O_{2max}$ reported here are from Tate et al. (30) with an additional five HA and five LA mice in WN and nine HA and nine LA mice in CH. Cold-induced $\dot{V}O_{2max}$ was determined by flowing heliox (21% O_2, 79% He or 12% O_2, 88% He), at 1,000 mL/min using mass flow meters and controllers (Sierra Instruments, Monterey, CA; MFC-4, Sable Systems, NV), through copper coils housed inside a temperature control cabinet and into a glass respirometry chamber (~500 mL) cooled to approximately −10°C. Heliox induces greater heat loss at warmer temperatures and avoids the risk of cold injury to the animals (40, 41). Mice were exposed to these conditions for ~15 min, and cold-induced $\dot{V}O_{2max}$ was defined as the peak value of $\dot{V}O_2$ averaged over a 10–15-s period (28, 42).

All mice were given at least 48 h to recover before another submaximal or cold-induced $\dot{V}O_2max$ trial was performed.

Stable Isotope Breath Analysis

Using indirect calorimetry can provide an estimate of whole body lipid oxidation rate. Although these rates are still very informative, they do not directly quantify the rate of oxidation of specific fuels or sources. We labelled endogenous fat stores with [^{13}C]palmitate and quantified rates of [^{13}C]palmitate oxidation by collecting exhaled $^{13}CO_2$ and measuring $\dot{V}CO_2$, as previously described for other species (43, 44). Using this approach, we could quantify how the rate of oxidation of labelled lipid stores specifically varied with ancestry, acclimation, or acute thermal challenge. Briefly, labelled food was prepared by completely dissolving 0.5 g of [1-^{13}C] palmitic acid (Cambridge Isotope Laboratories, Inc) in 95% ethanol to coat 0.5 kg of rodent chow (front and back). The

chow was then baked at 60°C overnight. A subset of mice was fasted up to a maximum of 24 h with full access to water to heavily deplete endogenous lipid stores (45, 46). After the 24-h fast, or once mouse weight was ~80% of their original body mass, animals were provided the ^{13}C-labelled chow for at least 10 days to replenish and ensure sufficient labeling of endogenous lipid stores. Mice were given labelled chow until all breath sampling trial data were collected.

Breath samples were collected from animals before and after [^{13}C]palmitic acid enrichment of fat stores. Food was removed 4 h before collection of breath $^{13}CO_2$ to prevent recently ingested ^{13}C from influencing our determination of endogenous lipid use (47). During respirometry trials at 30°C and 0°C, a 12-mL subsample of excurrent air was collected from these mice using a gas-tight glass syringe and transferred to a 12-mL glass exetainer (Labco). Breath samples were analyzed for δ^{13}C signatures by cavity ring-down spectroscopy using the Picarro G2201-I Isotopic Analyzer (Picarro, Inc., Santa Clara, CA). Using the techniques and equations provided by Dick et al. (48) and McCue et al. (43), δ^{13}C signatures were used to calculate [^{13}C]palmitic acid oxidation (44).

Measurement of Plasma Fatty Acids

Blood samples were obtained from the submandibular vein immediately following indirect calorimetry trials at 30°C and 0°C. Blood was immediately centrifuged at 10,000 g for 5 min to separate red cells from plasma. Plasma was quickly frozen in liquid nitrogen and stored until further analysis. To quantify free fatty acids, 20 μL of plasma were combined with 10 μL of internal standard (C17:0, 0.6 mg/mL) in 1 mL of 2,2-dimethoxypropane and vortexed. This was followed by the addition of 40 μL of HCl (12 M) and the methylation of free fatty acids was left to proceed for 1 h. The reaction was stopped with the addition of 20 μL of pyridine and vortexed. Next, 750 μL of iso-octane and 500 μL of dH$_2$O were added to the samples, and then centrifuged at 10,000 g for 5 min. The resultant upper phase was transferred to a new tube, and the process was repeated for the bottom layer. The top phases were combined and completely dried under N$_2$. The sample was resuspended in 50 μL of iso-octane and transferred to an autosampler tube. Another 50 μL of iso-octane was added to the original sample tube to resuspend any remaining contents and was also transferred to the autosampler tube and was completely dried under N$_2$. The final sample was resuspended in 50 μL of iso-octane (49).

Samples were analyzed using an Agilent Technologies 6890 N gas chromatograph with a 30 m fused silica capillary column (DB-23, Agilent Technologies), flame ionization detector and equipped with an automatic injection system (Agilent Technologies 7683B Series). Helium was used as the carrier gas at a constant pressure and column velocity of 44 cm/s, with 4 μL of sample injected into the column. The conditions used during analysis were the following: oven temperature initially programmed for 4 min at 160°C, ramped to 220°C at a rate of 2°C/min, and held at 220°C for 2 min, then ramped to 240°C at 10°C/min, and held at 240°C for 7 min. Postrun was 130°C for 4 min. The detector temperature was 250°C. Identities of fatty acid methyl esters were compared with the retention times of a standard FAME mix

(C8-C24, Sigma). We excluded analysis of fatty acids less than 16 carbons as we did not attempt to minimize volatilization (50).

Statistics

Linear mixed effects models were used to test for effects of population, acclimation, and experimental temperature. Analyses were performed using the lme4 package (51) in R v4.0.0 (52). We assessed the potential interactions between fixed factors, including body mass as a covariate and the random effects of family, sex, and age. If the variance explained by random effects did not approach significance ($P > 0.05$), we removed them and reran the analysis. Except for body mass, all other dependent variables were reduced to three-way analysis of variance (ANOVA)s, with mass as a covariate where appropriate. In addition, within each experimental temperature (30°C and 0°C), and cold-induced $\dot{V}_{O_{2max}}$ condition (normoxia and hypoxia), two-way ANOVAs were performed assessing the interaction between population and acclimation. Pairwise, Holm Sidak post hoc tests were performed to assess significant interactions (53). All statistical analyses were performed on the absolute values of the traits that were not corrected for body mass, but some data are presented as relative to body mass by convention to the literature ($\dot{V}_{O_2}$, $\dot{V}_{O_{2max}}$, ventilatory volumes, [^{13}C]palmitate oxidation, lipid oxidation, and thermal conductance). All data are presented as means ± SE. A statistical significance value was set at $P < 0.05$.

◼ RESULTS

Body Mass

White-footed mice weighed 29% more than both HA and LA deer mice, regardless of the acclimation environment ($P < 0.05$; Table 1). However, there was no significant difference in mass between HA and LA deer mice ($P > 0.05$; Table 1).

Respiration in Thermoneutral and Moderate Cold Temperatures

To determine if altitude ancestry or acclimation to CH influences metabolic rate during submaximal thermogenesis, we measured $\dot{V}_{O_2}$ at thermoneutrality (30°C) and during a moderate cold exposure (0°C) in LA and HA deer mice and white-footed mice. We found that $\dot{V}_{O_2}$ was threefold greater at 0°C compared with 30°C for all individuals, regardless of

population and acclimation environment ($P < 0.05$). HA and LA deer mice had greater $\dot{V}_{O_2}$ than white-footed mice at both 30°C and 0°C ($P < 0.05$), but there were no differences in $\dot{V}_{O_2}$ between HA and LA deer mice ($P > 0.05$). Furthermore, acclimation did not significantly influence $\dot{V}_{O_2}$ ($P > 0.05$; Fig. 1A). We calculated RER during these submaximal rates of thermogenesis and found it was unaffected by ambient temperature ($P > 0.05$). Although all mice tested at 0°C had similar RERs regardless of population or acclimation ($P > 0.05$), at 30°C white-footed mice acclimated to CH had higher RER than those housed in WN ($P < 0.05$). The range of RERs observed in all trials were between 0.70 and 0.80 across all groups, suggesting that lipids were the primary source of fuel in thermoneutral conditions and with moderate cold exposure (Fig. 1B).

Whole Animal Lipid Oxidation Rates during Submaximal Thermogenesis

Since lipid oxidation is the primary fuel for both shivering and nonshivering thermogenesis in rodents (15, 26), we determined if altitude ancestry or acclimation environment influenced this trait under moderate cold conditions. Using indirect calorimetry, we calculated whole animal lipid oxidation rates and observed an increase from 30°C to 0°C ($P < 0.05$). Across all temperatures, LA deer mice had greater lipid oxidation rates compared with white-footed mice ($P < 0.05$), but not compared with HA deer mice ($P > 0.05$). At 30°C, both HA and LA deer mice had greater lipid oxidation rates compared with white-footed mice ($P < 0.05$). Interestingly, CH acclimation did not affect whole animal rates of lipid oxidation ($P > 0.05$; Fig. 2A).

Thermal Conductance during Submaximal Thermogenesis

Thermal conductance was calculated to determine if changes in rates of heat loss occurred due to exposure to colder ambient temperatures with CH acclimation (Table 1). We found that thermal conductance was reduced as ambient temperature decreased from 30°C to 0°C ($F_{1,79} = 147.67$, $P < 0.001$), while controlling for any influence of body mass ($F_{1,79} = 21.16$, $P < 0.001$). Across all temperatures, white-footed mice had greater thermal conductance compared with HA and LA deer mice ($F_{2,79} = 16.43$, $P < 0.001$), which led to greater changes in body temperature after moderate cold exposure ($P < 0.05$). Acclimation to CH had no effect on thermal conductance ($F_{1,79} = 0.866$, $P = 0.355$; Table 1).

Table 1. *Body mass, change in body temperature, and thermal conductance of first-generation laboratory born and raised highland and lowland Peromyscus mice, acclimated to control (23°C, 21 kPa O$_2$; WN) or cold hypoxia (5°C, 12 kPa O$_2$; CH), exposed to ambient temperatures of 30°C and 0°C*

	Lowland (*P. leucopus*)				Lowland (*P. maniculatus*)				Highland (*P. maniculatus*)			
	Warm normoxia		Cold hypoxia		Warm normoxia		Cold hypoxia		Warm normoxia		Cold hypoxia	
	30°C	0°C	30°C	0°C	30°C	0°C	30°C	0°C	30°C	0°C	30°C	0°C
Mass, g	21.7 ± 1.7†	23.6 ± 1.6†	26.3 ± 0.6†	26.6 ± 0.9†	20.4 ± 1.2	19.9 ± 1.2	16.9 ± 0.6	17.2 ± 0.6	20.5 ± 1.3	20.7 ± 1.2	18.4 ± 0.7	18.8 ± 0.8
ΔT$_b$, °C	−0.31 ± 0.5	−2.11 ± 0.9†	0.61 ± 0.61	−1.04 ± 0.4†	0.64 ± 0.33	0.57 ± 0.33	1.24 ± 0.35	0.18 ± 0.27	0.13 ± 0.42	0.60 ± 0.35	0.93 ± 0.56	1.24 ± 0.45
C, mL·O$_2$·g^{-1}·h^{-1}·°C^{-1}	0.28 ± 0.01†	0.17 ± 0.01*†	0.24 ± 0.01†	0.16 ± 0.01*†	0.39 ± 0.02	0.23 ± 0.02*	0.39 ± 0.02	0.23 ± 0.01*	0.39 ± 0.03	0.20 ± 0.01*	0.39 ± 0.03	0.20 ± 0.02*

Values are presented as means ± SE. C, thermal conductance; ΔT$_b$, body temperature; WN, warm normoxia. Symbols representing significant differences result from Holm Sidak post hoc tests ($P < 0.05$). †Significantly different from highland and lowland deer mice within a given test temperature. *Significantly different from 30°C.
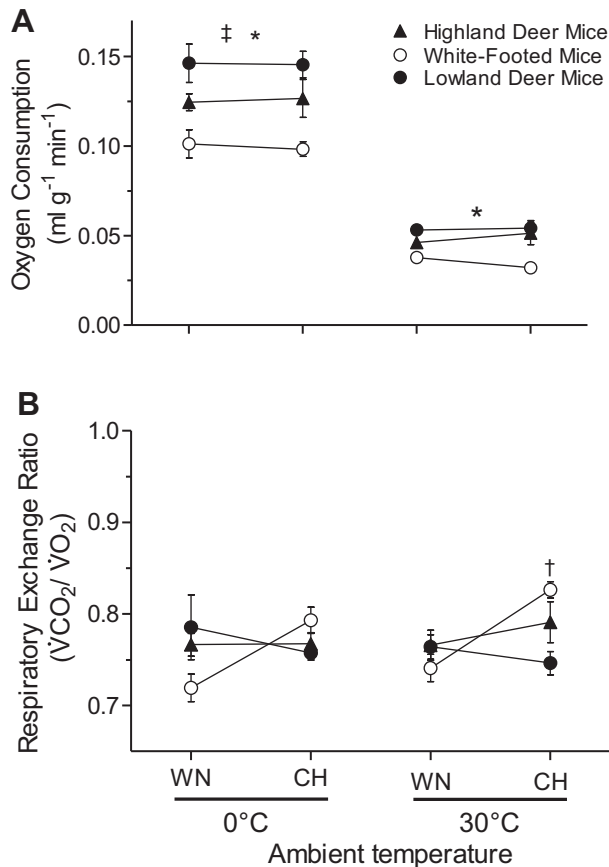
Figure 1. Oxygen consumption ($\dot{V}O_2$) (in mL·g^{-1}·min^{-1}) (*A*) and respiratory exchange ratio (RER = $\dot{V}CO_2/\dot{V}O_2$) (*B*) of first-generation laboratory born and raised highland and lowland *Peromyscus mice*, acclimated to control warm normoxia (23°C, 21 kPa O$_2$; WN) or cold hypoxia (5°C, 12 kPa O$_2$; CH), and then exposed acutely to ambient temperatures of 30°C and 0°C. *A*: $\dot{V}O_2$ showed a significant effect of ambient temperature ($F_{1,79}$ = 376.12, $P < 0.001$) and population ($F_{2,79}$ = 11.48, $P < 0.001$), while controlling for differences in body mass ($F_{1,79}$ = 16.08, $P < 0.001$). At 0°C, there was a significant population effect ($F_{2,39}$ = 5.69, $P = 0.007$). At 30°C, there was a main effect of population on $\dot{V}O_2$ ($F_{2,39}$ = 7.59, $P = 0.002$). *B*: for RER, there was a significant population x acclimation interaction ($F_{2,80}$ = 6.12, $P = 0.003$). At 30°C, there was a significant population x acclimation interaction ($F_{2,40}$ = 4.33, $P = 0.020$). Symbols representing significant differences result from Holm Sidak post hoc tests ($P < 0.05$). ‡Significant difference between test temperatures. *Highland and lowland deer mice are significantly different from white-footed mice. †Significant difference between CH lowlanders and CH white-footed mice at 30°C. $n = 5$ for WN and CH white-footed mice; $n = 10$ and 9 for WN and CH lowland deer mice, respectively; $n = 9$ and 8 for WN and CH highland deer mice, respectively. Data are presented as means ± SE. $\dot{V}CO_2$, CO$_2$ production.

[^{13}C]Palmitic Acid Oxidation

We directly quantified the oxidation of an individual fatty acid by labelling the fat stores in a subset of LA and HA deer mice using [^{13}C]palmitate and trapping exhaled ^{13}CO$_2$ during submaximal thermogenic trials. We found, similar to whole animal lipid oxidation, that [^{13}C]palmitate oxidation rates increased threefold as ambient temperatures declined from 30°C to 0°C ($P < 0.05$). However, in contrast to whole animal lipid oxidation rates, CH acclimation led to an increase in [^{13}C]palmitate oxidization ($P < 0.05$). Specifically, at 30°C

[^{13}C]palmitate oxidation increased in CH-acclimated HA mice compared with their WN controls ($P < 0.05$; Fig. 2*B*).

Circulating Plasma Nonesterified Fatty Acids

To understand if substrate use was reflected in changes of circulating plasma nonesterified fatty acids (NEFAs), we determined levels of total and individual circulating NEFAs (Fig. 2*C* and Fig. 3). Overall, plasma concentrations of total circulating NEFAs did not change as ambient temperature decreased ($P > 0.05$), nor were there any significant effects of population ($P > 0.05$) or acclimation ($P > 0.05$; Fig. 2*C*).

Similar to total NEFA, plasma concentrations of palmitate (16:0) and stearate (18:0) showed no differences between populations, acclimation or with changes in ambient temperature ($P > 0.05$; Fig. 3, *A* and *C*). In contrast, palmitoleate (16:1) was ~47% higher in LA deer mice than HA deer mice at 30°C ($P < 0.05$). The concentration of palmitoleate was also significantly higher in CH acclimated mice at 0°C ($P < 0.05$; Fig. 3*B*). Elaidate (18:1n9t) concentrations were found to be higher in HA deer mice, whereas oleate (18:1n9c) concentrations were higher in LA deer mice ($P < 0.05$; Fig. 3, *D* and *E*). Concentrations of oleate were also significantly greater in CH-acclimated mice at 0°C but significantly greater in WN animals at 30°C ($P < 0.05$; Fig. 3*E*). Linoleate (18:2n6c) concentrations were relatively constant with no significant effect of acclimation or temperature ($P > 0.05$); however, generally HA mice had higher levels of linoleate compared with LA mice ($P < 0.05$; Fig. 3*F*).

Whole Animal Lipid Oxidation at Cold-Induced $\dot{V}O_{2max}$

Thermogenic capacity was assessed by measuring cold-induced $\dot{V}O_{2max}$. We determined $\dot{V}O_2$ and lipid oxidation rates at $\dot{V}O_{2max}$ in both normoxia and hypoxia. After accounting for differences in body mass ($F_{1,135}$ = 16.93, $P < 0.001$), we found that $\dot{V}O_{2max}$ was higher in normoxia compared with hypoxia ($F_{1,135}$ = 353.22, $P < 0.001$). After CH acclimation, $\dot{V}O_{2max}$ increased ($F_{1,135}$ = 201.44, $P < 0.001$), but there were no significant population differences ($F_{2,135}$ = 2.80, $P = 0.064$; Fig. 4*A*).

RER at $\dot{V}O_{2max}$ was higher in normoxia compared with hypoxia ($F_{1,136}$ = 9.46, $P < 0.001$). There was a significant population × acclimation × test condition interaction in RER ($F_{1,136}$ = 3.80, $P = 0.025$), where WN HA mice tested in normoxia had greater RERs than WN HA mice, CH white-footed mice and WN white-footed mice when tested in hypoxia ($P < 0.05$). In normoxia, there was a significant population × acclimation interaction ($F_{2,40}$ = 4.10, $P = 0.024$), where CH acclimation led to a decrease in RER in HA mice ($P < 0.05$), whereas WN LA mice had lower RERs than WN HA mice ($P < 0.05$). In hypoxia, RER was not different among populations or with the acclimation environment (Fig. 4*B*).

Whole animal lipid oxidation rates at $\dot{V}O_{2max}$ were higher in normoxia compared with hypoxic conditions ($P < 0.05$). In addition, mice acclimated to CH had greater lipid oxidation rates compared with WN individuals ($P < 0.05$). In normoxia, HA deer mice acclimated to CH displayed higher lipid oxidation rates compared with WN white-footed mice ($P < 0.05$). In hypoxia, HA deer mice had higher lipid oxidation rates than LA mice, and CH acclimation led to an increase lipid oxidation ($P < 0.05$; Fig. 4*C*).

DISCUSSION

The main objective of this study was to determine the substrate utilization necessary to support both moderate and maximal intensities of thermogenesis in LA and HA native *Peromyscus* mice and how this utilization is influenced by acclimation to CH, simulating high altitude. We found that both deer mice and white-footed mice significantly increase whole body lipid oxidation rates from thermoneutral (30°C) to moderate cold (0°C) to support heat production. At 0°C, lipid oxidation accounted for the majority of total $\dot{V}O_2$ but did not differ among the three mouse populations. There was also no effect of CH acclimation on the proportional use of lipid oxidation at this moderate cold exposure. However,

when the oxidation of a major circulating free fatty acid was measured directly through $^{13}CO_2$ production, we found CH acclimation led to a significant increase in palmitate oxidation at 30°C when compared with WN acclimated controls. At cold-induced $\dot{V}O_{2max}$ under hypoxia, we found whole animal lipid oxidation rates were elevated two- to fourfold above moderate cold in WN and CH acclimated HA deer mice, respectively. This population also showed a significant effect of CH acclimation leading to higher whole animal lipid oxidation at $\dot{V}O_{2max}$ in normoxia. These results demonstrate that lipid oxidation is the major fuel supporting thermogenesis in deer mice, even at maximal cold-induced metabolic rates. Indeed, rates of lipid oxidation that support heat production at 0°C are similar or greater than maximal rates observed during moderate exercise intensities (20). Furthermore, oxidation rates to support maximal thermogenesis were 2.5- to 5.2-fold greater than maximal rates of lipid oxidation during exercise (6; Fig. 5) and the highest mass-specific lipid oxidation rates reported for any mammal (15, 20, 54, 55).

Submaximal and Maximal Thermogenic Metabolism

Thermoregulation allows for endotherms to balance rates of heat production and heat loss to maintain consistent body temperatures (3). To maintain stable body temperatures as ambient temperatures decrease, there must be an increase of both $\dot{V}O_2$ and substrate availability to match the increased metabolic demand of thermoregulation (28, 31). We observed as the need for heat generation increased, there was an increase in metabolic rate, but RERs remained constant and between 0.7 and 0.8 in all mice. Mice also showed a decline in thermal conductance that reduced rates of heat loss as ambient temperature decreased from thermoneutral (30°C) to moderate cold (0°C) temperatures (Fig. 1; Table 1), consistent with previous studies on small mammals (34, 56–59).
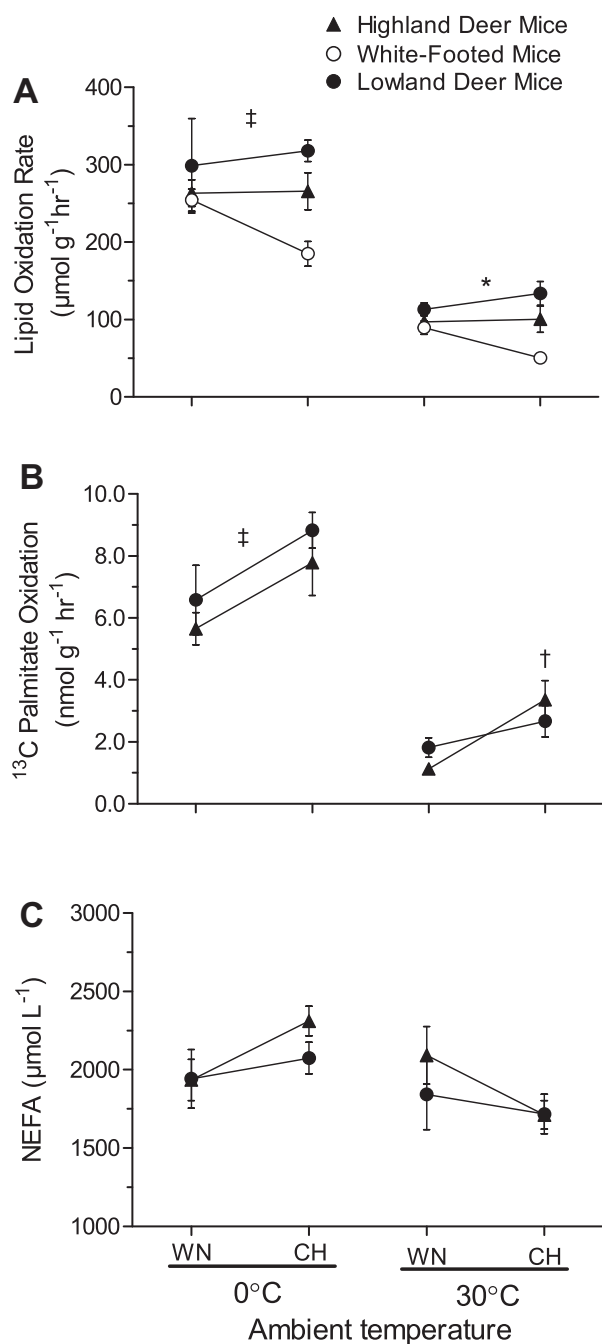
Figure 2. Whole animal lipid oxidation rates (in μmol·g^{-1}·h^{-1}) (*A*), rates of [^{13}C]palmitate oxidation (in nmol·g^{-1}·h^{-1}) (*B*), and concentrations of circulating plasma nonesterified fatty acids (NEFAs, in μmol·L^{-1}) (*C*) of first-generation laboratory born and raised highland and lowland *Peromyscus mice*, acclimated to control warm normoxia (23°C, 21 kPa O$_2$; WN) or cold hypoxia (5°C, 12 kPa O$_2$; CH), and exposed acutely to ambient temperatures of 30°C and 0°C. *A*: whole animal lipid oxidation rate showed a significant effect of ambient temperature ($F_{1,79} = 123.77$, $P < 0.001$) and population ($F_{2,79} = 3.51$, $P = 0.035$) while controlling for differences in body mass ($F_{1,79} = 3.95$, $P = 0.050$). At 30°C, there was a significant population effect ($F_{2,39} = 5.88$, $P = 0.006$) while controlling for body mass ($F_{1,39} = 0.236$, $P = 0.630$). *B*: [^{13}C]palmitate oxidation showed a significant effect of ambient temperature ($F_{1,35} = 157.30$, $P < 0.001$) and acclimation ($F_{1,35} = 12.21$, $P = 0.001$) while controlling for body mass ($F_{1,35} = 0.044$, $P = 0.835$). At 30°C, there was a significant population x acclimation interaction ($F_{1,17} = 6.59$, $P = 0.020$), and significant acclimation effect ($F_{1,17} = 14.82$, $P = 0.001$), all while controlling for body mass ($F_{1,17} = 0.000$, $P = 0.999$). Symbols representing significant differences result from Holm Sidak post hoc tests ($P < 0.05$). ‡Significant difference between test temperatures. *Highland and lowland deer mice are significantly different from white-footed mice. †Significant difference between highland acclimation groups at 30°C. *A*: $n = 5$ for WN and CH white-footed mice; $n = 10$ and 9 for WN and CH lowland deer mice, respectively; $n = 9$ and 8 for WN and CH highland deer mice, respectively. *B*: $n = 7$ and 5 for WN and CH lowland deer mice, respectively; $n = 8$ and 4 for WN and CH highland deer mice, respectively. *C*: $n = 8$–9 for WN and 5 for CH lowland deer mice, respectively; $n = 9$–10 and 4 for WN and CH highland deer mice, respectively. All data are presented as means ± SE.
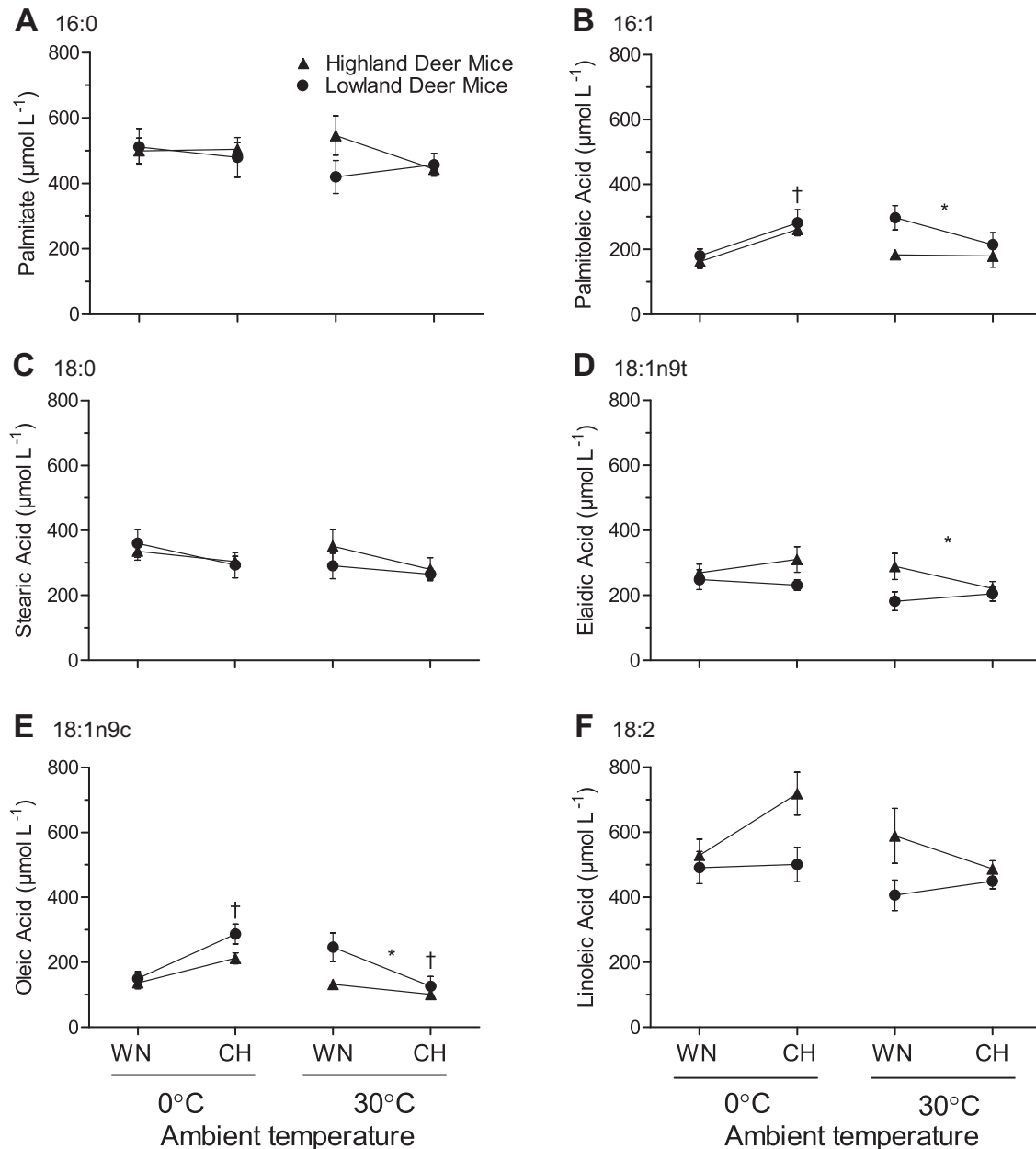
Figure 3. Concentrations of individual plasma fatty acids (in µmol/L) of first-generation laboratory born and raised highland and lowland deer mice (*Peromyscus maniculatus*), acclimated to control warm normoxia (23°C, 12 kPa O_2; WN) or cold hypoxia (5°C, 12 kPa O_2; CH), acutely exposed to ambient temperatures of 30°C and 0°C. Palmic acid (16:0) (*A*); Palmitoleic acid (16:1) (*B*); at 0°C, there was a significant acclimation effect ($F_{1,23} = 12.99$, $P = 0.001$), whereas at 30°C, there was a significant population effect ($F_{1,23} = 6.70$, $P = 0.015$). Stearic acid (18:0) (*C*); Elaidic acid (18:1n9t) (*D*); at 30°C, there was a significant population effect ($F_{1,23} = 4.96$, $P = 0.036$). Oleic acid (18:1n9c) (*E*); at 0°C, there was a significant acclimation effect ($F_{1,23} = 19.66$, $P < 0.001$), whereas at 30°C, there was a significant population effect ($F_{1,23} = 5.77$, $P = 0.025$) and acclimation effect ($F_{1,23} = 4.91$, $P = 0.037$). Linoleic acid (18:2) (*F*); Symbols representing significant differences result from Holm Sidak post hoc tests ($P < 0.05$). *Main population effect within a given test temperature. †Main acclimation effect within a given test temperature. $n = 8$–9 for WN and 5 for CH lowland deer mice, respectively; $n = 9$–10 and 4 for WN and CH highland deer mice, respectively. Data are presented as means ± SE.

Interestingly, when exposed to moderate cold, both HA and LA deer mice had the same $\dot{V}O_2$ and RERs, suggesting a specific amount of energy and fuel required for submaximal thermogenic demand, which was maintained even after acclimation to CH.

When cold-induced $\dot{V}O_{2max}$ was stimulated, RER remained low suggesting fuel utilization did not change between moderate and maximal thermogenic requirements, despite the large change in metabolic rate (Fig. 4, *A* and *B*). Previous research has shown an adaptive advantage for high aerobic capacity in HA deer mice (25), and that wild HA mice maintain higher hypoxic $\dot{V}O_{2max}$ than their LA conspecifics when tested in their native environments (27). We did not find a significant difference in thermogenic capacity between laboratory born and raised HA and LA mice (Fig. 4*A*). These results are consistent with previous measurements of

hypoxic $\dot{V}_{O_{2max}}$ in WN and CH acclimated deer mice ([28], [30]). However, when deer mice were acclimated to warm hypoxia, HA mice did show higher hypoxic $\dot{V}_{O_{2max}}$ than both LA deer mice ([28]), and white-footed mice ([30]). Although the combined effects of cold hypoxia can have opposing effects on thermogenesis in laboratory mice ([12]), we found CH acclimation significantly increased $\dot{V}_{O_{2max}}$ in all populations. Given the evidence that higher thermogenic capacities are under directional selection in deer mice at high altitude ([25]), having the ability to elevate thermogenic capacity in response to cold would be adaptive for surviving alpine environments.

Whole Animal Lipid Oxidation Rates

The substrates used by mammals to support thermogenesis, and the rate they are oxidized to support heat production,
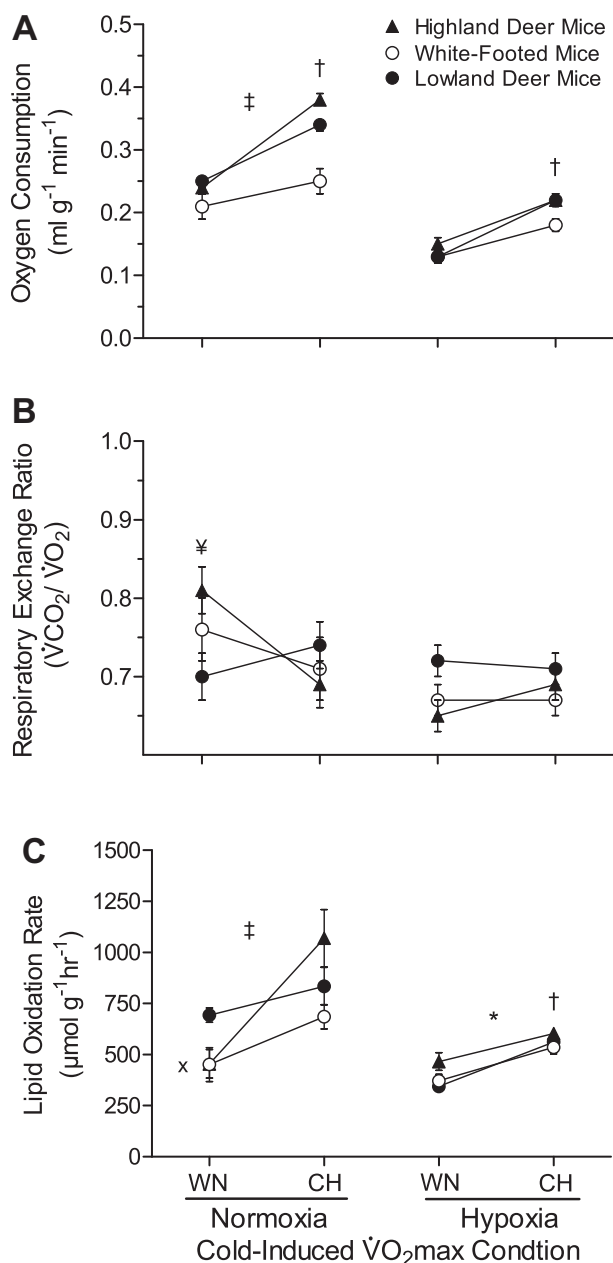
has received little attention. Here we provide data on substrate use during moderate cooling and at peak thermogenesis in *Peromyscus*. All mice fueled submaximal thermogenesis primarily with lipids, which contributed between 70 and 93% of total metabolism. At thermoneutrality, lipids supported only 59% of total energy requirements in white-footed mice after CH acclimation (Fig. 1*B*). Nonetheless, these mice used lipid oxidation to a proportionally greater extent to power thermogenesis than previously observed in rats exposed to 5°C (Fig. 5; [44]).

During moderate rates of thermogenesis, lipid oxidation rates were equivalent to maximal rates observed during aerobic locomotion in the same species (Fig. 5; [37]). Data from a number of low altitude native mammals (humans, mice rats, goats, and dogs) show that substrate use during exercise follows a predictable pattern, where rates of lipid oxidation plateau at moderate intensities ([60]). At higher exercise intensities, lipid use does not increase, even when fatty acid availability is artificially increased ([19]). However, we show that during thermogenesis in deer mice, lipid oxidation continues to increase and support higher metabolic rates to levels that are fivefold higher than those observed during exercise in this species (Fig. 5). These high rates of lipid oxidation support both the activation of BAT metabolism and

Figure 4. Cold-induced maximal oxygen consumption ($\dot{V}_{O_2}$) (in mL·g^{-1}·min^{-1}) (*A*) with the corresponding respiratory exchange ratios (RER = $\dot{V}_{CO_2}/\dot{V}_{O_2}$) (*B*) and whole animal lipid oxidation rates (in µmol·g^{-1}·h^{-1}) (*C*) of first-generation laboratory born and raised highland and lowland *Peromyscus* mice, acclimated to control warm normoxia (23°C, 21 kPa O_2; WN) or cold hypoxia (5°C, 12 kPa O_2; CH), acutely exposed to normoxia (21% O_2) or hypoxia (12% O_2). *A*: there was a significant effect of condition on cold-induced $\dot{V}_{O_{2max}}$ ($F_{1,135} = 353.22$, $P < 0.001$) while controlling for the effects of body mass ($F_{1,135} = 16.93$, $P < 0.001$). White-footed mice weighed significantly more than both highland and lowland deer mice, regardless of the acclimation environment ($P < 0.05$). There was a significant effect of acclimation on cold-induced $\dot{V}_{O_{2max}}$ under normoxic ($F_{1,39} = 48.85$, $P < 0.001$) and hypoxic ($F_{1,95} = 170.33$, $P < 0.001$) conditions. *B*: under normoxic conditions, there was a significant population × acclimation interaction in RER ($F_{2,40} = 4.10$, $P = 0.024$). *C*: lipid oxidation rates showed a significant effect of $\dot{V}_{O_{2max}}$ condition ($F_{1,135} = 43.74$, $P < 0.001$) and acclimation ($F_{1,135} = 55.00$, $P < 0.001$). There was a significant interaction between population, acclimation, and $\dot{V}_{O_{2max}}$ conditions ($F_{1,135} = 6.93$, $P = 0.001$). All factors had mass as a covariate ($F_{1,135} = 6.33$, $P = 0.013$). In normoxia, there was a significant interaction between population and acclimation ($F_{2,39} = 4.62$, $P = 0.016$) while controlling for mass ($F_{1,39} = 0.202$, $P = 0.656$). In hypoxia, there was a significant effect of population ($F_{2,95} = 3.16$, $P = 0.047$) and acclimation ($F_{1,95} = 44.06$, $P < 0.001$) while controlling for differences in body mass ($F_{1,95} = 16.68$, $P < 0.001$). Symbols representing significant differences result from Holm Sidak post hoc tests ($P < 0.05$). ‡Significant difference between cold-induced $\dot{V}_{O_{2max}}$ conditions. *Highlanders significantly differ from lowland deer mice within hypoxic cold-induced $\dot{V}_{O_{2max}}$ conditions. †Main acclimation effect within a given cold-induced $\dot{V}_{O_{2max}}$ condition. ¥WN highland deer mice significantly differ from CH highland and WN lowland deer mice, within the normoxic $\dot{V}_{O_{2max}}$ condition. ×WN highlanders and WN white-footed mice significantly differ from CH highlanders within the normoxic $\dot{V}_{O_{2max}}$ condition. $n = 5$–15 for WN white-footed mice [mass (in g) = 24.8 ± 1.7 and 26.5 ± 1.0 for normoxia and hypoxia, respectively] and CH white-footed mice [mass (in g) = 27.6 ± 1.7 and 26.7 ± 1.0 for normoxia and hypoxia, respectively]. $n = 9$–19 for WN lowland deer mice [mass (in g) = 20.8 ± 1.2 and 20.7 ± 1.0 for normoxia and hypoxia, respectively] and CH lowland deer mice [mass (in g) = 17.9 ± 1.3 and 20.2 ± 0.9 for normoxia and hypoxia, respectively]. $n = 8$–21 for WN highland deer mice [mass (in g) = 22.0 ± 1.3 and 20.3 ± 0.8 for normoxia and hypoxia, respectively] and CH highland deer mice [mass (in g) = 19.5 ± 1.3 and 21.5 ± 0.9 for normoxia and hypoxia, respectively]. Data are presented as means ± SE. Mass and $\dot{V}_{O_{2max}}$ in hypoxia data from Tate et al. ([30]). $\dot{V}_{CO_2}$, CO_2 production.
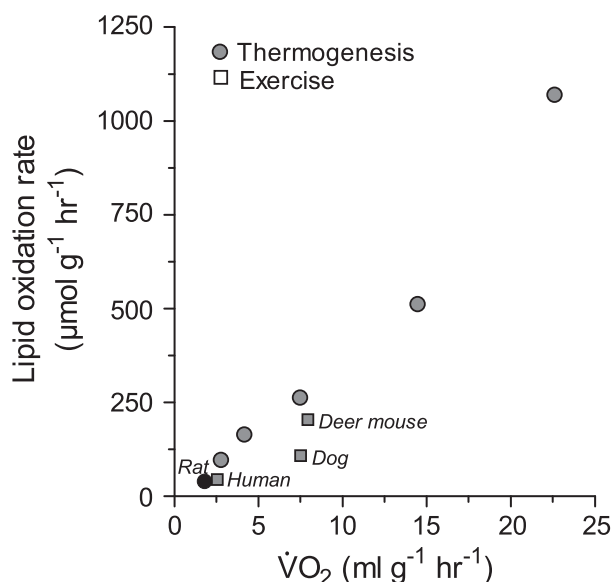
Figure 5. Mass-specific lipid oxidation rates as a function of metabolic rate at 30°C, 15°C, and 0°C and normoxic cold-induced $\dot{V}O_{2max}$ in warm normoxia (23°C, 21 kPa O_2) and cold hypoxia (5°C, 12 kPa O_2) acclimated high-altitude deer mice (this study) compared with those during submaximal aerobic exercise in running humans (54), dogs (55), and deer mice (20) and with moderate shivering thermogenesis in rats (dark circle represents lipid oxidation but only during shivering thermogenesis) (15).

high rates of muscle shivering. The degree that these tissues rely on either endogenous or circulatory sources of lipid fuel is currently unclear. It is important to note that we determined lipid oxidation by indirect calorimetry, which can become unreliable when animals leave steady state conditions at higher metabolic rates (55). However, given the linear relationship between $\dot{V}O_2$ and total ventilation across a range of thermogenic intensities (58) and ventilatory equivalents that never reach anaerobic threshold (61, 62), our data suggest that thermoregulating mice in this study were in steady state metabolism, even at cold-induced $\dot{V}O_{2max}$ (Supplemental Fig. S1 and Supplemental Tables S1 and S2; Supplemental Material for this article can be found online at https://doi.org/10.6084/m9.figshare.13564784).

The oxidation of [13C]palmitate was also directly quantified during moderate cold exposures. From thermoneutral to moderate cold, we observed a threefold increase of [13C]palmitate oxidation (Fig. 2B), directly reflecting the increase in whole animal lipid oxidation (Fig. 2A). However, although total lipid oxidation was unaffected by acclimation in HA mice, [13C]palmitate oxidation was higher in CH acclimated HA mice. Interestingly, plasma concentrations of palmitate did not track changes in its oxidation but remained stable with acute changes in temperature and with CH acclimation (Fig. 3A). This mismatch between whole body palmitate oxidation and circulating palmitate concentrations with thermogenic demand may shed some light on how fatty acids are utilized to match demand for heat production. Although difficulty in interpreting experimentally induced changes in blood metabolites has been highlighted by others (63), we suggest two potential explanations for our data. The first explanation suggests that rates of palmitate disappearance into active tissues are tightly matched with rates of appearance into plasma.

The second explanation suggests CH leads to greater use of palmitate from endogenous lipid stores within thermo-effector tissues, such as muscle and/or BAT. Measuring flux of circulating fatty acids, along with the oxidation of both circulatory and intracellular sources of lipid will provide a deeper understanding of how lipid depots are used during thermogenesis.

Total plasma NEFA levels also remained constant, a reflection of changes in those individual fatty acids with high percent contributions to total NEFA (e.g., palmitate and stearate; Fig. 2C and Fig. 3). However, HA mice showed higher plasma concentrations of elaidate and linoleate, but lower concentrations of palmitoleate and oleate, compared with LA deer mice (Fig. 3). Acclimation to CH led to a selective increase in plasma levels of palmitoleate and oleate at 0°C and a decrease in oleate at 30°C. These findings suggest a population, acclimation, and temperature-specific mobilization of specific NEFA in deer mice.

At peak rates of thermogenesis, lipids were the predominant fuel used by all mice, regardless of altitude ancestry. Lipids constituted 67 to 100% to total oxygen use, regardless of the acclimation environment (Fig. 4B). In hypoxia, highlanders showed higher lipid oxidation rates than lowland deer mice at $\dot{V}O_{2max}$, which further increased with CH acclimation (Fig. 4C). The capacity for high rates of lipid oxidation is likely an important feature of the HA phenotype, and along with an elevated $\dot{V}O_{2max}$ (25), increases the probability of winter survival in HA deer mice. Similar to differences in $\dot{V}O_{2max}$ (27), lipid oxidation in hypoxia was higher in HA deer mice due to a combined effect of phenotypic plasticity, overlaid upon genetic differences in maximal rates of fuel use. When the constraint of hypoxia was removed and thermogenic capacity was determined in normoxia, lipid oxidation at $\dot{V}O_{2max}$ increased with CH in highlanders, to the highest mass-specific rates recorded for any mammal (Fig. 4C).

Mice used proportionally more lipids in hypoxia than in normoxia, with this fuel accounting for almost 100% of $\dot{V}O_2$ in some instances. These observations may appear paradoxical, given the higher ATP yield per mole of O_2 afforded by carbohydrate oxidation (14, 64) and their increased use with exercise observed in highland native mice (17, 20). However, the efficiency advantage of carbohydrates as a fuel is likely outweighed by the need of critical tissues for this limited resource (33). Instead, mobilization and utilization of lipids is increased in response to a prolonged need for metabolic heat production, even in the face of low O_2 availability. Lipid reserves are in abundance in mammals (49) and could sustain prolonged thermogenesis at an ecologically relevant alpine ambient temperature of 0°C (Western Regional Climate Centre), for up to 71 h, assuming ~4 g of stored lipids (20% of a 20-g mouse). Our findings also suggest that even at maximal rates of heat production, onboard lipids would last up to 16 h until fully depleted. These liberal estimates assume all lipids are accessible to the thermo-effector tissues. Nevertheless, mice are capable of oxidizing lipids at very high rates by delivering fatty acids to working mitochondria. How this process occurs is a fruitful area of future research.

The Lipid Oxidation Pathway

Elevated rates of lipid oxidation to support moderate and maximal rates of heat production require sufficient capacities

for mobilization, transport, and oxidation to supply free fatty acids to working mitochondria. During exercise, maximal lipid oxidation is thought to be limited by fatty acid uptake across the sarcolemma of working muscle (24, 65) and mitochondrial membranes (66, 67). Both of these potential limitations may be bypassed during thermogenesis. Unlike exercise, where skeletal muscle accounts for ~80% of O_2 and substrate use (68), thermogenesis in small mammals involves both shivering by skeletal muscle and nonshivering thermogenesis, principally in BAT. Perhaps thermogenic tissues increase reliance on intracellular stores of lipids for fueling thermogenesis. For example, BAT increases intracellular lipolysis with cold stress in both humans and rats (9, 10, 69). Alternatively, cold stress may stimulate increased blood flow and increased capacity for fatty acid uptake for BAT and shivering muscle (70). Acclimation to CH would further amplify these differences by increasing BAT activity and increasing capacity for lipid transport and oxidation in BAT and muscle. Thus, differences in fuel use between exercise and thermogenesis may involve the relative contributions of these energy consuming tissues involved (6, 47). Indeed, further research is needed to understand the mechanisms involved and determine how these components of the lipid oxidation pathway are regulated during thermogenesis.

PERSPECTIVES AND SIGNIFICANCE

We report that lipid oxidation is the primary fuel supporting both moderate and maximal rates of thermogenesis in both deer mice and white-footed mice. Rates of lipid oxidation also reflect the higher thermogenic capacity in hypoxia of HA deer mice, suggesting capacity for high lipid use has also evolved in this environment. In addition, we show that rates of lipid oxidation during thermogenesis are much higher than during exercise and report the highest mass-specific rates, observed in any land-dwelling mammal, to our knowledge. These results highlight a need to understand how lipid oxidation is regulated during high rates of metabolic heat production. For example, it is unknown how the limitation to maximal lipid oxidation observed during exercise is circumvented when animals are thermoregulating. We suggest the increased reliance on BAT activity is an important driver for the high reliance on lipid use during thermogenesis; however, NST occurring in BAT accounts for ~50%–60% of cold-induced $\dot{V}O_{2max}$ in deer mice (13), suggesting lipids used for shivering is more than twice that is observed during exercise (20). Rates of lipid use by shivering muscles are likely much higher than those observed during exercise. How these higher rates of oxidation are achieved are currently unclear. Animals in chronically cold environments, such as the high alpine, would also require a consistent supply of dietary nutrients to maintain the observed elevated daily metabolic rates (5). However, we know little about food sources available to HA deer mice or how they may differ from those at lower elevations. These next steps will provide a deeper understanding of how thermoregulation can raise the ceiling for fat oxidation, and ultimately provide more insight as to how these deer mice can survive the challenging environment of high-altitude.

DISCLOSURES

No conflicts of interest, financial or otherwise, are declared by the authors.

AUTHOR CONTRIBUTIONS

S.A.L. and G.B.M. conceived and designed research; S.A.L. and K.B.T. performed experiments; S.A.L. and K.C.W. analyzed data; S.A.L. and G.B.M. interpreted results of experiments; S.A.L. and G.B.M. prepared figures; S.A.L. and G.B.M. drafted manuscript; S.A.L., K.B.T., K.C.W., and G.B.M. edited and revised manuscript; S.A.L., K.B.T., K.C.W., and G.B.M. approved final version of manuscript.

REFERENCES

1. **Fristoe TS**, **Burger JR**, **Balk MA**, **Khaliq I**, **Hof C**, **Brown JH.** Metabolic heat production and thermal conductance are mass-independent adaptations to thermal environment in birds and mammals. *Proc Natl Acad Sci USA* 112: 15934–15939, 2015. doi:10.1073/pnas.1521662112.

2. **Khaliq I**, **Fritz SA**, **Prinzinger R**, **Pfenninger M**, **Böhning-Gaese K**, **Hof C.** Global variation in thermal physiology of birds and mammals: Evidence for phylogenetic niche conservatism only in the tropics. *J Biogeogr* 42: 2187–2196, 2015. doi:10.1111/jbi.12573.

3. **Scholander PF**, **Hock R**, **Walters V**, **Irving L.** Adaptation to cold in arctic and tropical mammals and birds in relation to body temperature, insulation, and basal metabolic rate. *Biol Bull* 99: 259–271, 1950. doi:10.2307/1538742.

4. **Chappell MA**, **Hammond KA.** Maximal aerobic performance of deer mice in combined cold and exercise challenges. *J Comp Physiol B Biochem B* 174: 41–48, 2004. doi:10.1007/s00360-003-0387-z.

5. **Hayes JP.** Altitudinal and seasonal effects on aerobic metabolism of deer mice. *J Comp Physiol B* 159: 453–459, 1989. doi:10.1007/BF00692417.

6. **Foster DO**, **Frydman ML.** Tissue distribution of cold-induced thermogenesis in conscious warm- or cold-acclimated rats reevaluated from changes in tissue blood flow: the dominant role of brown adipose tissue in the replacement of shivering by nonshivering thermogenesis. *Can J Physiol Pharmacol* 57: 257–270, 1979. doi:10.1139/y79-039.

7. **Cannon B**, **Nedergaard J.** Brown adipose tissue: function and physiological significance. *Physiol Rev* 84: 277–359, 2004. doi:10.1152/physrev.00015.2003.

8. **Haman F**, **Legault SR**, **Weber JM.** Fuel selection during intense shivering in humans: EMG pattern reflects carbohydrate oxidation. *J Physiol* 556: 305–313, 2004. doi:10.1113/jphysiol.2003.055152.

9. **Blondin DP**, **Labbé SM**, **Phoenix S**, **Guérin B**, **Turcotte ÉE**, **Richard D**, **Carpentier AC**, **Haman F.** Contributions of white and brown adipose tissues and skeletal muscles to acute cold-induced metabolic responses in healthy men. *J Physiol* 593: 701–714, 2015. doi:10.1113/jphysiol.2014.283598.

10. **Labbé SM**, **Caron A**, **Bakan I**, **Laplante M**, **Carpentier AC**, **Lecomte R**, **Richard D.** In vivo measurement of energy substrate contribution to cold-induced brown adipose tissue thermogenesis. *FASEB J* 29: 2046–2058, 2015. doi:10.1096/fj.14-266247.

11. **Nespolo RF**, **Opazo JC**, **Rosenmann M**, **Bozinovic F.** Thermal acclimation, maximum metabolic rate, and nonshivering thermogenesis of *Phyllotis xanthopygus* (Rodentia) in the Andes mountains. *J Mammal* 80: 742–748, 1999. doi:10.2307/1383243.

12. **Beaudry JL**, **McClelland GB.** Thermogenesis in CD-1 mice after combined chronic hypoxia and cold acclimation. *Comp Biochem Physiol B Biochem Mol Biol* 157: 301–309, 2010. doi:10.1016/j.cbpb.2010.07.004.

13. **Van Sant MJ**, **Hammond KA.** Contribution of shivering and nonshivering thermogenesis to thermogenic capacity for the deer mouse (*Peromyscus maniculatus*). *Physiol Biochem Zool* 81: 605–611, 2008. doi:10.1086/588175.

14. **Weber JM.** Metabolic fuels: regulating fluxes to select mix. *J Exp Biol* 214: 286–294, 2011. doi:10.1242/jeb.047050.

15. **Vaillancourt E**, **Haman F**, **Weber JM.** Fuel selection in Wistar rats exposed to cold: Shivering thermogenesis diverts fatty acids from re-esterification to oxidation. *J Physiol* 587: 4349–4359, 2009. doi:10.1113/jphysiol.2009.175331.

16. **Brooks GA**, **Mercier J.** Balance of carbohydrate and lipid utilization during exercise: the "crossover" concept. *J Appl Physiol* 76: 2253–2261, 1994. doi:10.1152/jappl.1994.76.6.2253.

17. **Schippers MP**, **Ramirez O**, **Arana M**, **Pinedo-Bernal P**, **McClelland GB.** Increase in carbohydrate utilization in high-altitude Andean mice. *Curr Biol* 22: 2350–2354, 2012. doi:10.1016/j.cub.2012.10.043.

18. **Weber JM**, **Haman F.** Oxidative fuel selection: adjusting mix and flux to stay alive. *Int Congr Ser* 1275: 22–31, 2004. doi:10.1016/j.ics.2004.09.043.

19. **Hargreaves M**, **Kiens B**, **Richter EA.** Effect of increased plasma free fatty acid concentration on muscle metabolism in exercising men. *J Appl Physiol (1985)* 70: 194–201, 1991. doi:10.1152/jappl.1991.70.1.194.

20. **Lau DS**, **Connaty AD**, **Mahalingam S**, **Wall N**, **Cheviron ZA**, **Storz JF**, **Scott GR**, **McClelland GB.** Acclimation to hypoxia increases carbohydrate use during exercise in high-altitude deer mice. *Am J Physiol Regul Integr Comp Physiol* 312: R400–R411, 2017. doi:10.1152/ajpregu.00365.2016.

21. **Templeman NM**, **Schutz H**, **Garland T**, **McClelland GB.** Do mice bred selectively for high locomotor activity have a greater reliance on lipids to power submaximal aerobic exercise? *Am J Physiol Regul Integr Comp Physiol* 303: R101–R111, 2012. doi:10.1152/ajpregu.00511.2011.

22. **Hayes AJP**, **Chappell MA**, **Hayes JP**, **Chappell MA.** Individual consistency of maximal oxygen consumption in deer mice. *Funct Ecol* 4: 495–503, 1990. doi:10.2307/2389317.

23. **McClelland GB**, **Lyons SA**, **Robertson CE.** Fuel use in mammals: Conserved patterns and evolved strategies for aerobic locomotion and thermogenesis. *Integr Comp Biol* 57: 231–239, 2017. doi:10.1093/icb/icx075.

24. **Weber JM**, **Brichon G**, **Zwingelstein G**, **McClelland G**, **Saucedo C**, **Weibel ER**, **Taylor CR.** Design of the oxygen and substrate pathways. IV. Partitioning energy provision from fatty acids. *J Exp Biol* 199: 1667–1674, 1996.

25. **Hayes JP**, **O'Connor CS.** Natural selection on thermogenic capacity of high-altitude deer mice. *Evolution* 53: 1280–1287, 1999. doi:10.2307/2640830.

26. **Cheviron ZA**, **Bachman GC**, **Connaty AD**, **McClelland GB**, **Storz JF.** Regulatory changes contribute to the adaptive enhancement of thermogenic capacity in high-altitude deer mice. *Proc Natl Acad Sci USA* 109: 8635–8640, 2012. doi:10.1073/pnas.1120523109.

27. **Cheviron ZA**, **Connaty AD**, **McClelland GB**, **Storz JF.** Functional genomics of adaptation to hypoxic cold-stress in high-altitude deer mice: Transcriptomic plasticity and thermogenic performance. *Evolution* 68: 48–62, 2014. doi:10.1111/evo.12257.

28. **Tate KB**, **Ivy CM**, **Velotta JP**, **Storz JF**, **McClelland GB**, **Cheviron ZA**, **Scott GR.** Circulatory mechanisms underlying adaptive increases in thermogenic capacity in high-altitude deer mice. *J Exp Biol* 220: 3616–3620, 2017. doi:10.1242/jeb.164491.

29. **Lui MA**, **Mahalingam S**, **Patel P**, **Connaty AD**, **Ivy CM**, **Cheviron ZA**, **Storz JF**, **McClelland GB**, **Scott GR.** High-altitude ancestry and hypoxia acclimation have distinct effects on exercise capacity and muscle phenotype in deer mice. *Am J Physiol Regul Integr Comp Physiol* 308: R779–R791, 2015. doi:10.1152/ajpregu.00362.2014.

30. **Tate KB**, **Wearing OH**, **Ivy CM**, **Cheviron ZA**, **Storz JF**, **McClelland GB**, **Scott GR.** Coordinated changes across the O2 transport pathway underlie adaptive increases in thermogenic capacity in high-altitude deer mice. *Proc Biol Sci* 287: 20192750, 2020. doi:10.1098/rspb.2019.2750.

31. **McClelland GB**, **Scott GR.** Evolved mechanisms of aerobic performance and hypoxia resistance in high-altitude natives. *Annu Rev Physiol* 81: 561–583, 2019. doi:10.1146/annurev-physiol-021317-121527.

32. **Moriya K**, **Leblanc J**, **Arnold J.** Effects of exercise and intermittent cold exposure on shivering and nonshivering thermogenesis in rats. *Jpn J Physiol* 37: 715–727, 1987. doi:10.2170/jjphysiol.37.715.

33. **McClelland GB**, **Hochachka PW**, **Weber J-M.** Carbohydrate utilization during exercise after high-altitude acclimation: a new perspective. *Proc Natl Acad Sci USA* 95: 10288–10293, 1998. doi:10.1073/pnas.95.17.10288.

34. **Chappell MA**, **Holsclaw DS.** Effects of wind on thermoregulation and energy balance in deer mice (*Peromyscus maniculatus*). *J Comp Physiol B* 154: 619–625, 1984. doi:10.1007/BF00684416.

35. **White CR**, **Portugal SJ**, **Martin GR**, **Butler PJ.** Respirometry: Anhydrous drierite equilibrates with carbon dioxide and increases washout times. *Physiol Biochem Zool* 79: 977–980, 2006. doi:10.1086/505994.

36. **Withers PC.** Measurement of VO₂, VCO₂, and evaporative water loss with a flow-through mask. *J Appl Physiol Respir Environ Exerc Physiol* 42: 120–123, 1977. doi:10.1152/jappl.1977.42.1.120.

37. **Frayn KN.** Calculation of substrate oxidation rates in vivo from gaseous exchange. *J Appl Physiol Respir Environ Exerc Physiol* 55: 628–634, 1983. doi:10.1152/jappl.1983.55.2.628.

38. **Bulow J.** Lipid mobilization and utilization. In: *Principles of Exercise Biochemistry*, edited by Poort JR**.** Basel, Switzerland: Karger, 1988.

39. **Gessaman JA**, **Nagy K.** Energy metabolism: errors in gas-exchange conversion factors. *Physiol Zool* 61, 1988. https://www.jstor.org/stable/30156159.

40. **Chappell MA**, **Rezende EL**, **Hammond KA.** Age and aerobic performance in deer mice. *J Exp Biol* 206: 1221–1231, 2003. doi:10.1242/jeb.00255.

41. **Rosenmann MS**, **Morrison PR.** Maximum oxygen consumption and heat loss facilitation in small homeotherms by He-O2. *Am J Physiol* 226: 490–495, 1974. doi:10.1152/ajplegacy.1974.226.3.490.

42. **Robertson CE**, **McClelland GB.** Developmental delay in shivering limits thermogenic capacity in juvenile high-altitude deer mice (*Peromyscus maniculatus*). *J Exp Biol* 222: jeb210963, 2019. doi:10.1242/jeb.210963.

43. **McCue MD**, **McWilliams SR**, **Pinshow B.** Ontogeny and nutritional status influence oxidative kinetics of nutrients and whole-animal bioenergetics in zebra finches, *Taeniopygia guttata*: New applications for ¹³C breath testing. *Physiol Biochem Zool* 84: 32–42, 2011. doi:10.1086/657285.

44. **McCue MD**, **Welch KC.** ¹³C-Breath testing in animals: theory, applications, and future directions. *J Comp Physiol B* 186: 265–285, 2016. doi:10.1007/s00360-015-0950-4.

45. **McCue MD**, **Pollock ED.** Measurements of substrate oxidation using ¹³CO2-breath testing reveals shifts in fuel mix during starvation. *J Comp Physiol B Biochem B* 183: 1039–1052, 2013. doi:10.1007/s00360-013-0774-z.

46. **Sokolović M**, **Wehkamp D**, **Sokolović A**, **Vermeulen J**, **Gilhuijs-Pederson LA**, **van Haaften RIM**, **Nikolsky Y**, **Evelo CTA**, **van Kampen AHC**, **Hakvoort TBM**, **Lamers WH.** Fasting induces a biphasic adaptive metabolic response in murine small intestine. *BMC Genomics* 8: 361–318, 2007. doi:10.1186/1471-2164-8-361.

47. **Mccue MD**, **Voigt CC**, **Jefimow M**, **Wojciechowski MS.** Thermal acclimation and nutritional history affect the oxidation of different classes of exogenous nutrients in Siberian hamsters, *Phodopus sungorus*. *J Exp Zool A Ecol Genet Physiol* 321: 503–514, 2014. doi:10.1002/jez.1882.

48. **Dick MF**, **Alcantara-Tangonan A**, **Oghli YS**, **Welch KC.** Metabolic partitioning of sucrose and seasonal changes in fat turnover rate in ruby-throated hummingbirds (*Archilochus colubris*). *J Exp Biol* 223: jeb212696, 2020. doi:10.1242/jeb.212696.

49. **McClelland GB**, **Hochachka PW**, **Weber JM.** Effect of high-altitude acclimation on NEFA turnover and lipid utilization during exercise in

rats. *Am J Physiol Endocrinol Metab* 277: E1095–E1102, 1999. doi:10.1152/ajpendo.1999.277.6.E1095.

50. **Price ER**, **Armstrong C**, **Guglielmo CG**, **Staples JF.** Selective mobilization of saturated fatty acids in isolated adipocytes of hibernating 13-lined ground squirrels *Ictidomys tridecemlineatus*. *Physiol Biochem Zool* 86: 205–212, 2013. doi:10.1086/668892.

51. **Bates D**, **Mächler M**, **Bolker BM**, **Walker SC.** Fitting linear mixed-effects models using lme4. *J Stat Softw* 67, 2015. doi:10.18637/jss.v067.i01.

52. **Team RC.** R: A Language and Environment for Statistical Computing [Online]. Wienna, Austria: R Foundation for Statistical Computing, 2013. [http://www.r-project.org].

53. **Hothorn T**, **Bretz F**, **Westfall P.** Simultaneous inference in general parametric models. *Biom J* 50: 346–363, 2008. doi:10.1002/bimj.200810425.

54. **Achten J**, **Venables MC**, **Jeukendrup AE.** Fat oxidation rates are higher during running compared with cycling over a wide range of intensities. *Metabolism* 52: 747–752, 2003. doi:10.1016/S0026-0495(03)00068-4.

55. **Roberts TJ**, **Weber JM**, **Hoppeler H**, **Weibel ER**, **Taylor CR.** Design of the oxygen and substrate pathways. II. Defining the upper limits of carbohydrate and fat oxidation. *J Exp Biol* 199: 1651–1658, 1996.

56. **Casey TM**, **Withers PC**, **Casey KK.** Metabolic and respiratory responses of arctic mammals to ambient temperature during the summer. *Comp Biochem Physiol* 64: 331–341, 1979. doi:10.1016/0300-9629(79)90452-3.

57. **Chappell MA.** Effects of ambient temperature and altitude on ventilation and gas exchange in deer mice (*Peromyscus maniculatus*). *J Comp Physiol B* 155: 751–758, 1985. doi:10.1007/BF00694590.

58. **Rezende EL**, **Chappell MA**, **Hammond KA.** Cold-acclimation in Peromyscus: temporal effects and individual variation in maximum metabolism and ventilatory traits. *J Exp Biol* 207: 295–305, 2004. doi:10.1242/jeb.00760.

59. **Withers PC**, **Casey TM**, **Casey KK.** Allometry of respiratory and haematological parameters of arctic mammal. *Comp Biochem Phyiol A* 64: 343–350, 1979. doi:10.1016/0300-9629(79)90453-5.

60. **Schippers MP**, **LeMoine CMR**, **McClelland GB.** Patterns of fuel use during locomotion in mammals revisited: the importance of aerobic scope. *J Exp Biol* 217: 3193–3196, 2014. doi:10.1242/jeb.099432.

61. **Newstead CG.** The relationship between ventilation and oxygen consumption in man is the same during both moderate exercise and shivering. *J Physiol* 383: 455–459, 1987. doi:10.1113/jphysiol.1987.sp016420.

62. **Yu CCW**, **McManus AM**, **Li AM**, **Sung RYT**, **Armstrong N.** Cardiopulmonary exercise testing in children. *Hong Kong J Paediatr* 15: 35–47, 2010. doi:10.1378/chest.120.1.81.

63. **McCue MD**, **Albach A**, **Salazar G.** Previous repeated exposure to food limitation enables rats to spare lipid stores during prolonged starvation. *Physiol Biochem Zool* 90: 63–74, 2017. doi:10.1086/689323.

64. **Brand MD.** The stoichiometry of proton pumping and synthesis in mitochondria. *Biochem (Lond)* 16: 20–24, 1994. https://www.researchgate.net/publication/248022370_The_stoichiometry_of_proton_pumping_and_ATP_synthesis_in_mitochondria.

65. **Weibel ER**, **Taylor CR**, **Weber JM**, **Vock R**, **Roberts TJ**, **Hoppeler H.** Design of the oxygen and substrate pathways. VII. Different structural limits for oxygen and substrate supply to muscle mitochondria. *J Exp Biol* 199: 1699–1709, 1996.

66. **Båvenholm PN**, **Pigon J**, **Saha AK**, **Ruderman NB**, **Efendic S.** Fatty acid oxidation and the regulation of malonyl-CoA in human muscle. *Diabetes* 49: 1078–1083, 2000. doi:10.2337/diabetes.49.7.1078.

67. **Stephens FB.** Does skeletal muscle carnitine availability influence fuel selection during exercise? *Proc Nutr Soc* 77: 11–19, 2018. doi:10.1017/S0029665117003937.

68. **Armstrong RB**, **Essen-Gustavsson B**, **Hoppeler H**, **Jones JH**, **Kayar SR**, **Laughlin MH**, **Lindholm A**, **Longworth KE**, **Taylor CR**, **Weibel ER.** O$_2$ delivery at VO$_2$max and oxidative capacity in muscles of standardbred horses. *J Appl Physiol (1985)* 73: 2274–2282, 1992. doi:10.1152/jappl.1992.73.6.2274.

69. **Blondin DP**, **Labbé SM**, **Noll C**, **Kunach M**, **Phoenix S**, **Guérin B**, **Turcotte ÉE**, **Haman F**, **Richard D**, **Carpentier AC.** Selective impairment of glucose but not fatty acid or oxidative metabolism in brown adipose tissue of subjects with type 2 diabetes. *Diabetes* 64: 2388–2397, 2015. doi:10.2337/db14-1651.

70. **Blondin DP**, **Frisch F**, **Phoenix S**, **Guérin B**, **Turcotte ÉE**, **Haman F**, **Richard D**, **Carpentier AC.** Inhibition of intracellular triglyceride lipolysis suppresses cold-induced brown adipose tissue metabolism and increases shivering in humans. *Cell Metab* 25: 438–447, 2017. doi:10.1016/j.cmet.2016.12.005.